

# The global variation in the iron isotope composition of marine hydrogenetic ferromanganese deposits: implications for seawater chemistry?

S. Levasseur<sup>a,\*</sup>, M. Frank<sup>a</sup>, J.R. Hein<sup>b</sup>, A.N. Halliday<sup>a</sup>

<sup>a</sup>*Institute of Isotope Geology and Mineral Resources, Department of Earth Sciences, ETH Zentrum NO CO 61, Sonneggstrasse 5, CH-8092 Zürich, Switzerland*

<sup>b</sup>*U.S. Geological Survey, 345 Middlefield Road, Menlo Park, CA 94025, USA*

Received 16 December 2003; received in revised form 4 May 2004; accepted 7 May 2004

## Abstract

The iron (Fe) isotope compositions of 37 hydrogenetic ferromanganese deposits from various oceans have been analysed by MC-ICPMS; they permit the construction of a global map of Fe isotopic values. The isotopic compositions range between  $-1.2$  and  $-0.1$ ‰ in  $\delta^{57}\text{Fe}_{\text{IRMM14}}$ . Averages for the Atlantic and the Pacific are  $-0.41$  and  $-0.88$ ‰, but their standard deviations are identical ( $0.27$ ,  $1\sigma$ ) and the data very largely overlap. No correlation is found with Pb or Nd isotope compositions and there is no evidence that the observed oceanic Fe isotopic heterogeneity is directly controlled by variations in continental sources. The small quantities of Fe that can be introduced from hydrothermal sources render as unlikely the possibility that the isotopic variations reflect variable proportions of continental and hydrothermal Fe, as recently proposed. The more likely explanation is that the variations are induced locally within the ocean. The exact sources of fractionation remain unclear. Likely possibilities are the dissolution and reprecipitation processes that liberate Fe from sediments during anoxic events, dissolution in surface waters or processes occurring during growth of the crusts.

© 2004 Elsevier B.V. All rights reserved.

**Keywords:** iron isotopes; manganese crusts; atmospheric input; hydrothermal input; intraoceanic processes

## 1. Introduction

Iron (Fe) is a bio-limiting micronutrient in high nutrient low chlorophyll (HNLC) areas—those regions of the oceans in which nutrients are not fully consumed by phytoplankton [1] ([2] for more

recent developments). The biogeochemical cycle of iron (Fe) in the oceans can thus influence marine productivity and can affect the draw down of atmospheric  $\text{CO}_2$  by photosynthetic marine organisms. It is therefore important to improve our knowledge of the mechanisms that control the fluxes of Fe from the continents and the cycling of iron in the oceans. Iron isotopes provide a promising new tool for such studies. However, because of analytical limitations, natural variations in Fe isotopic composition have only recently been studied. The direct

\* Corresponding author. Tel.: +41-1-632-07-31; fax: +41-1-632-11-79.

E-mail address: [levasseur@erdw.ethz.ch](mailto:levasseur@erdw.ethz.ch) (S. Levasseur).

measurement of the isotopic composition of Fe in seawater is still a major challenge due to very low concentrations. Ferromanganese crusts have provided powerful records of variations in the isotopic composition of various elements dissolved in ocean deep waters. These variations, depending on the element, are a function of changes in paleocirculation, source provenances, style and intensity of weathering on the continents and changes in tectonic processes. Serial sampling of ferromanganese crusts provide useful insights into the history of the oceans in the past [3]. As such, studies of ferromanganese crust may yield invaluable information on marine Fe isotope systematics today and how this has changed with time.

The first attempt to reconstruct and interpret the evolution of iron isotopes in North Atlantic deep water [4] concluded that the isotopic variations were controlled by terrigenous inputs on the basis of a correlation between Pb and Fe isotopes over the past 6 million years. However, no geographical variations in the Fe isotope composition of hydrogenetic crusts have been published to provide confirmation of this interpretation. Intraocean variations of  $-1.39$  to  $0.66\text{‰}$  ( $\delta^{57}\text{Fe}$ ) have been reported for the present day from a set of ferromanganese crust surface scrapings, but no systematic difference between oceans was found [5]. Here we present a global dataset for hydrogenous (or hydrogenetic) crusts and nodules that provides a map for the modern ocean.

## 2. Samples and analytical methods

The sample set comprises 37 hydrogenous ferromanganese crusts, one ferromanganese nodule and one hydrothermal deposit. These were selected to achieve global coverage (Table 1, Fig. 1). The origin of the crusts has been established from the mineralogy, texture and geochemistry. The most recent layer of the crusts and nodules was sampled to a depth of about 0.5 mm. One hydrogenous crust (BM1969.05) was also sampled deeper at 0.5–0.8 and 0.8–1.6 mm. The hydrothermal deposit was analysed as a bulk sample. Unlike the crusts, the hydrothermal deposit formed below the seafloor–seawater interface. Analysis of the surface 0.5 mm of crusts averages any

effects of recent glacial and interglacial changes in erosion and in ocean chemistry. Therefore, they are only suitable for assessing long-term averaged controls on Fe isotope variation ( $\sim 50$ – $250$  kyr). Between 1 and 5 mg aliquots of sample powder were used for the analyses. The powder was leached overnight at room temperature in 1 ml of 6 N HCl. Any undissolved material was eliminated from the solution by centrifugation. The supernatant was evaporated in the presence of  $\text{H}_2\text{O}_2$  to ensure that all Fe is oxidized to Fe(III). The residue of evaporation was then redissolved in 6 N HCl. The solution was passed through a column containing about 0.5 ml of BioRad® AG1-X8, 200–400 mesh anion exchange resin. After elution of matrix elements with 3 ml of 6 N HCl, the Fe was eluted with 2 ml of 0.05 N HCl. The solution containing the Fe was evaporated and redissolved in 0.05 N HCl. This extraction procedure is quantitative and does not induce fractionation between Fe isotopes. This has been tested in different ways. First, the yield has been checked to be 100% ( $\pm 3\%$ ). Second, some IRMM-014 standard solutions were passed through the whole procedure, and their isotopic composition measured. Finally, some standard solutions containing similar amounts of Fe were added to the eluted matrix of a real sample, and then reprocessed as a natural sample. The standards always gave the expected value within uncertainty ( $\pm 0.13\text{‰}$ ), regardless of chemical treatment. Total procedural blanks were at the nanogram level. This is negligible when dealing with sample sizes in between 200  $\mu\text{g}$  and 1 mg of Fe.

The absence of fractionation generated by the leaching step was tested on GMAT-14D, a ferromanganese crust rich in detrital minerals [6]. The leachates obtained after 30, 90, 210 min and overnight have the same composition as the bulk (cf. Table 1). This shows first that the Fe contained in the detrital material has a negligible influence on the isotopic composition of the hydrogenous Fe, as this detrital material is expected to have a  $\delta^{57}\text{Fe}$  composition of  $0.11 \pm 0.14\text{‰}$  ( $2\sigma$ ) [7]; and second, that leaching with 6 N HCl does not induce a fractionation between Fe isotopes. Moreover, the negligible impact of Fe from the detrital component is confirmed by an XRD study [8] of the composition of seven crusts (four of which are also included in this work), which showed

Table 1  
Results of isotope analyses

Cruise or supplier	Sample	Section (mm)	Type	Location	Latitude	Longitude	Water depth (m)	$\delta^{57}\text{Fe}$ ‰	$2\sigma$	$\delta^{57}\text{Fe}^*$ ‰	$2\sigma$	$^{206}\text{Pb}/^{204}\text{Pb}$	$\epsilon\text{Nd}$	Growth rate (mm/Myr)
ALV539	D2-1A	0–1	Crust	NW Atlantic	35°36.4' N	58°47.1' W	2662	–0.36	0.05	–0.12 (–0.12)	0.06	19.267	–12.93	3.1 [35]
SO-154	52 CD-1	0–1	Crust	NW Atlantic	16°38.0' N	62°19.5' W	784.5	–0.28	0.06	–0.09 (–0.09)	0.01	18.970	–10.5	–
Arc1 TR079	D14	0–0.5	Crust	NW Atlantic	16°55.0' N	61°10.0' W	2000	–0.27	0.10	–0.10 (–0.09)	0.08	19.157	–12.54	2.9 [36]
Gosnold 65–75	2383	0–0.5	Crust	NW Atlantic	31°38' 00"N	78°40' 12"W	512	–0.85	0.14	–0.34 (–0.27)	0.17			–
	BM1963.897	0–0.5	Crust	NW Atlantic	30°50' 00"N	78°30' 00"W	850	–0.36	0.12	–0.09 (–0.12)	0.10	19.100	–11.00	4.5 [36]
Hudson St. 54	BM1969.05	0–0.5	Crust	NW Atlantic	39°00' 00"N	60°57' 00"W	1850	–0.72	0.14	–0.31 (–0.23)	0.20	19.210		1.6 [37]
		0.5–0.8						–0.68	0.07	–0.21 (–0.22)	0.15			
		0.8–1.6						–0.76	0.09	–0.16 (–0.24)	0.06			
Discovery 144	D10979	0–1	Crust	NE Atlantic	32°36.0' N	24°25.0' W	5347–4867	–0.42	0.06	–0.15 (–0.14)	0.05	19.003	–11.12	2.3 [36]
Discovery II	1966.069	0–0.5	Crust	NE Atlantic	42°54' 00"N	20°13' 00"W	3247	–0.10	0.01	–0.02 (–0.03)	0.1	–	–	–
VEMA CH78	DR01-001a	0–0.5	Crust	N Atlantic	10°35' 00"N	42°42' 00"W	3512	–0.23	0.08	–0.09 (–0.07)	0.07	18.954	–11.60	5.0
Atlantis II 96	D10-7	0–0.5	Crust	Central N Atlantic	23°38' 00"N	44°29' 00"W	2432	–0.07	0.06	0.04 (–0.02)	0.13	–	–	–
ROM96	S16 01–13	0–0.5	Crust	Eq. Atlantic	0°48' 20"S	20°35' 45"W	3200	–0.33	0.08	–0.09 (–0.11)	0.13	18.954	–11.74	5.5 [38]
ROM96	G9646–63	0–0.5	Crust	Eq. Atlantic	1°12' 30"S	28°31' 30"W	3350	–0.54	0.05	–0.15 (–0.17)	0.09	18.750	–9.5	1.4 [38]
ROM96	G9632–47	0–0.5	Crust	Eq. Atlantic	0°48' 56"S	21°01' 18"W	4710	–0.43	0.11	–0.15 (–0.14)	0.07	18.929	–10.40	0.6 [38]
SO-84	DS43	0–2	Crust	SE Atlantic	15°9.0' S	8°21.0' W	1990–1966	–0.27	0.11	–0.18 (–0.09)	0.09	19.092	–12.39	1.6 [36]
SO-84	DS43	Same powder						–0.28	0.08	–0.01 (–0.09)	0.20			
SO-84	DS43	0–0.5 (second sample)						–0.31	0.16	–0.15 (–0.10)	0.13			

(continued on next page)

Table 1 (continued)

Cruise or supplier	Sample	Section (mm)	Type	Location	Latitude	Longitude	Water depth (m)	$\delta^{57}\text{Fe}$ ‰	$2\sigma$	$\delta^{57}\text{Fe}^*$ ‰	$2\sigma$	$^{206}\text{Pb}/^{204}\text{Pb}$	$\epsilon\text{Nd}$	Growth rate (mm/Myr)
Endeavor EN 063	32D	0–1	Crust	SW Atlantic	32°11.5' S	32°43.0' W	3310	–0.95	0.06	–0.39 (–0.31)	0.06	18.773	–9.85	–
Endeavor EN 063	27D	0.1	Crust	SW Atlantic	32°52.0' S	32°13.0' W	3610	–0.41	0.06	–0.11 (–0.13)	0.19	18.750	–9.5	–
Circé	D140-3	0–0.5 (first sample)	Crust	S Atlantic	26°03' 36" S	5°42' 48" E	1800	–0.90	0.08	–0.26 (–0.29)	0.18	18.901	–10.00	–
Circé	D140-3	0–0.5 (second sample)						–0.97	0.09	–0.33 (–0.31)	0.13			
Circé	D219-7	0–0.5 (first sample)	Crust	SE Atlantic	7°26' 24" S	1°20' 52" W	4294	–0.15	0.05	–0.12 (–0.05)	0.15	19.020	–11.90	–
Circé	D219-7	0–0.5 (second sample)						–0.13	0.14	–0.04 (–0.05)	0.12			
Circé	219D	0–0.5	Crust	SE Atlantic	7°26' 24" S	1°20' 48" W	4410	–0.14	0.05	–0.11 (–0.05)	0.14	19.020	–11.90	–
Dodo	232D	0–0.5	Crust	Indian	5°23.0' S	97°29.0' E	4121	–0.86	0.05	–0.27 (–0.28)	0.10	18.919	–7.35	4.3
HEMS Mahabiss	96626 E(6)	0–0.5	Thin crust	Indian	1°26.0' S	66°34.0' E	3385	–0.69	0.08	–0.21 (–0.22)	0.11	18.758	–7.8	–
Antipode	145D-B1	0–0.5	Crust	Indian	7°20' 00" S	57°56' 18" E	2421	–0.90	0.08	–0.34 (–0.29)	0.11	–	–	–
Antipode	109D-C	0–0.5	Crust	Indian	27°58' 24" S	60°47' 42" E	5438	–0.52	0.10	–0.19 (–0.17)	0.10	–	–	2.9 [39]
Antipode	77D-C	0–0.5	Crust	Indian	18°20' 30" S	63°38' 24" E	3447	–0.35	0.10	–0.11 (–0.11)	0.10	–	–	–
ERDC	019D	0–0.5	Crust	Indian	8°37' 00" N	96°15' 00" E	449	–1.08	0.10	–0.34 (–0.35)	0.06			–
TBD 463	6854-6 bottom	0–0.5	Nodule	Southern Ocean	37°46' 30" S	16°55' 06" E	4517	–0.68	0.08	–0.17 (–0.22)	0.11	18.855	–9.01	3.9 [40]
TBD 463	6854-6 bottom	0–0.5						–0.63	0.07	–0.23 (–0.20)	0.05			
TBD 463	6854-6 top	0–0.5						–0.66	0.05	–0.30 (–0.21)	0.05			
	DR153	0–0.5	Crust	Southern Ocean	64°57' 30" S	91°16' 24" W	3225	–1.03	0.01	–0.26 (–0.33)	0.03	18.759	–7.90	0.7 [40]
	DR153							–0.99	0.05	–0.32 (–0.32)	0.07			–

F7 87-SC	D9-16	0–0.5	Crust	NE Pacific	32°15' 34.8" N	121°16' 21.6" W	2267	–1.06	0.01	–0.29 (–0.34)	0.10	18.845	–2.65	–
F10-89-CP	D11–16	0–0.5	Crust	Pacific	11°38' 54" N	161°40' 30" W	1780	–0.42	0.06	–0.19 (–0.14)	0.11	–	–	–
Challenger St. 253	M317	0–0.5	Crust	N Central Pacific	38°09.0' N	156°25.0' W	5715	–0.63	0.09	–0.21 (–0.20)	0.01	18.662	–3.58	–
Challenger St. 281	M353	0–0.5	Crust	S Central Pacific	22°21' 00" S	150°17' 00" W	4362	–0.15	0.08	–0.03 (–0.05)	0.10	–	–	–
CS-06-A	DR04	0–0.5	Hard ground Crust	Pacific	21°00' 28" S	152°51' 23" E	4080	–1.11	0.06	–0.41 (–0.36)	0.10	18.680	–1.10	–
PLDS II	St. 39 D4	0–0.5	Crust	Pacific	00°24' 48" N	86°05' 36" W	3000	–0.97	0.10	–0.37 (–0.31)	0.05	–	–	–
FDR75-3	D10-144	0–0.5	Crust	Pacific	17°09' 00" S	75°15' 42" W	4218	–0.82	0.06	–0.28 (–0.26)	0.04	–	–	–
F7-86-HW	CD29-2	0–0.5	Crust	Central Eq. Pacific	16°42' 24" N	168°14' 12" W	2180	–0.61	0.13	–0.14 (–0.20)	0.08	18.658	–3.70	2.1 [8]
S6-79-NP	D4-13A	0–0.5	Crust	NE Pacific	53°32' 36" N	144°22' 24" W	2100	–1.19	0.09	–0.39 (–0.38)	0.11	18.837	–2.02	1.7 [41]
GMAT	14D	30 min HCl 6 N	Crust	NE Pacific	13°59' 00" N	96°08' 00" W	1900	–0.83	0.05	–0.31 (–0.27)	0.02			
GMAT	14D	1 h 30 min HCl 6 N						–0.79	0.08	–0.25 (–0.25)	0.17			
GMAT	14D	3 h 30 min HCl 6 N						–0.78	0.12	–0.19 (–0.25)	0.11			
GMAT	14D	Overnight HCl 6 N						–0.81	0.04	–0.27 (–0.26)	0.11			
GMAT	14D	Overnight HCl 6 N (same powder)						–0.80	0.06	–0.18 (–0.26)	0.06			
GMAT	14D	Total dissolution						–0.79	0.06	–0.35 (–0.25)	0.20			
GMAT	14D	Mean						–0.80	0.04	–0.26 (–0.26)	0.13	18.703	–2.4	10.3 [8]
Pleiade II	D5-1A	0–0.5	Hydrothermal deposit	Galapagos ridge	0°36' N	86°08.82' W	3822	–1.69	0.02	–0.64 (–0.54)	0.15	18.849	–	–

$\delta^{57}\text{Fe} = [(^{57}\text{Fe}/^{54}\text{Fe})_{\text{sample}} / (^{57}\text{Fe}/^{54}\text{Fe})_{\text{standard}} - 1] \times 1000$  (‰),  $\delta^{57}\text{Fe}^* = [(^{57}\text{Fe}/^{56}\text{Fe})_{\text{sample}} / (^{57}\text{Fe}/^{56}\text{Fe})_{\text{standard}} - 1] \times 1000$  (‰). Parameters of the fractionation line between  $\delta^{57}\text{Fe}$  and  $\delta^{57}\text{Fe}^*$  using weighted least-square method are (with 95% confidence bounds):  $p_1 = 3.34$  (3.06, 3.63) and  $p_2 = -0.05$  (–0.11, 0.02), where  $\delta^{57}\text{Fe} = p_1 \times \delta^{57}\text{Fe}^* + p_2$ . The number in brackets in the  $\delta^{57}\text{Fe}^*$  column is the expected value for  $\delta^{57}\text{Fe}^*$ , assuming that  $\delta^{57}\text{Fe}$  is known. All the growth rates are determined from  $^{10}\text{Be}/^9\text{Be}$  except from the one from [39] which was dated by U/Th. The growth rates without references are unpublished data. Pd and Nd data come from [3].

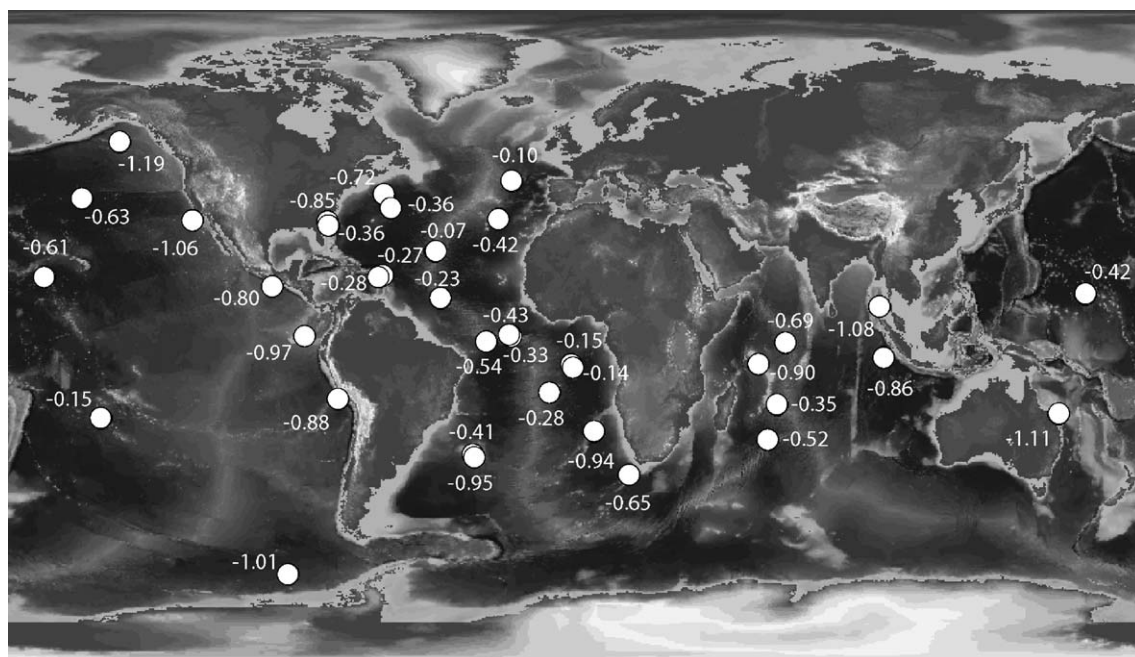


Fig. 1. Map of ferromanganese crust sample locations and the  $\delta^{57}\text{Fe}$  [‰ ; (O)] values of a surface scrapings from each crust.

that the content of detrital material is usually (a) quite low (a few percent) and (b) essentially free of Fe-bearing minerals (it mainly consists of quartz, plagioclase, calcite, etc.). This means that the influence of detrital Fe would be negligible even if it were completely extracted from the silicate minerals by the 6 N HCl leach, which is unlikely.

To test whether sample heterogeneity or, more specifically, short-term changes in isotopic composition were an issue, we also sampled several crusts and the nodule in the different places on their surfaces (see samples DS43, D140-3, D219-7 and 6854-6 in Table 1). The different subsamples gave identical results showing that the sampling size was large enough to be representative and that the crusts have been homogeneous over the time represented by the samples ( $\sim 50$ – $250$  kyr).

All Fe isotopic measurements were performed on a NuPlasma MC-ICPMS at the ETH Zürich, using a standard bracketing technique. Both the sample and the standard were in 0.05 N HCl solutions at concentrations between 6 and 8 ppm. The intensities of the beams generated by the standard and the samples were matched to within 15%. This permitted cancel-

lation of any bias induced by residual argide molecular interferences [9]. The four isotopes, 54, 56, 57 and 58, of iron were measured and the contributions of Cr and Ni were monitored using masses 53 and 60, respectively. These are negligible for our samples after chemical purification. Each analysis consisted of 20 measurements of two 5-s cycles, totaling approximately 10 min including the background measurement time, wash out and sample transfer time. The two cycles are required in order to use a Faraday cup at the low mass end of the array (L5) fitted with a  $10^{10}\Omega$  resistor. This permits the measurement of  $^{56}\text{Fe}$  with a signal of up to  $10^{-9}\text{A}$  for improved signal/background ratio without sacrificing other instrument applications.

All the Fe isotope data are reported relative to the iron isotopic standard IRMM-14 (Standard from the Institute for Reference Materials and Measurements, European Commission). The observed variations are expressed in  $\delta$  units (‰).

$$\delta^{57}\text{Fe} = \left[ \left( \frac{^{57}\text{Fe}}{^{54}\text{Fe}} \right)_{\text{sample}} / \left( \frac{^{57}\text{Fe}}{^{54}\text{Fe}} \right)_{\text{IRMM-14}} - 1 \right] \times 1000 (\text{‰})$$



and

$$\delta^{57}\text{Fe}^* = [({}^{57}\text{Fe}/{}^{56}\text{Fe})_{\text{sample}}/({}^{57}\text{Fe}/{}^{56}\text{Fe})_{\text{IRMM-14}} - 1] \times 1000(\text{‰})$$

$\delta^{57}\text{Fe}^*$  is only used to control the parameters of the fractionation line. We used  $\delta^{57}\text{Fe}^*$  because we did our measurements in two cycles;  ${}^{56}\text{Fe}$  being measured only together with  ${}^{57}\text{Fe}$ . The fit of the fractionation line achieved using a weighted least-square method to take into account the uncertainties on the measurements gives the following parameters (with 95% confidence bounds) for  $\delta^{57}\text{Fe} = a \times \delta^{57}\text{Fe}^* + b$ , where  $a = 3.36$  (3.06, 3.63) and  $b = -0.05$  (-0.11, 0.02). These are in good agreement with the expected line  $\delta^{57}\text{Fe} = 3.11 \times \delta^{57}\text{Fe}^*$ .

It should be noted that the normalization to IRMM-14 used here is shifted from the one based on the igneous Fe baseline adopted by some authors [10]. The  $\delta^{57}\text{Fe}$  value of IRMM-14 relative to the igneous Fe baseline =  $-0.11 \pm 0.14 \text{‰}$  ( $2\sigma$ ) [7]. This means that  $\delta^{57}\text{Fe}_{\text{IRMM14}} = \delta^{57}\text{Fe}_{\text{IGNEOUS}} + 0.11$ . The long-term reproducibility of our internal laboratory standard (a solution formed from a dissolved hematite mineral) is  $\delta^{57}\text{Fe} 0.86 \pm 0.13 \text{‰}$  ( $2\sigma$ ,  $n = 129$ ) over the period of measurement of the samples presented here.

### 3. Results

All the iron isotope data discussed below will be expressed in  $\delta^{57}\text{Fe}_{\text{IRMM14}}$ ; data expressed in  $\delta^{56}\text{Fe}$  normalized to “bulk earth Fe baseline” have been corrected for interlaboratory bias using a  $\delta^{56}\text{Fe}$  value of  $-0.09 \text{‰}$  relative to the “bulk earth Fe baseline” as proposed in [10] and then converted to  $\delta^{57}\text{Fe}$ . The observed spread in the data is rather large compared to the variations observed in other natural samples [7]: the analyses of a large variety of continental sedimentary rocks showed only slightly more variability than the observed in the volcanic and plutonic rocks ( $0.11 \pm 0.15 \text{‰}$  from [10]). In contrast, the variability of Fe isotope compositions we observed in hydrogenous crust surfaces (recent growth) is between  $-1.2$  and  $-0.1 \text{‰}$ . This is a slightly smaller range than that

determined for another set of ferromanganese crust samples [5], which ranges from  $+0.7$  to  $-1.4 \text{‰}$ . The composition is independent of the growth rate (Fig. 2).

In contrast to the global ocean distribution observed for Pb and Nd isotopes, there is no clear trend between the oceans for Fe isotopes [3] (Fig. 3). The samples from the Atlantic Ocean have a mean of  $-0.41 \pm 0.27 \text{‰}$  ( $1\sigma$ ) whereas the other oceans have lower mean values of  $-0.74 \pm 0.54 \text{‰}$  ( $1\sigma$ ; for the Indian Ocean),  $-0.83 \pm 0.25 \text{‰}$  ( $1\sigma$ ; for the Southern Ocean) and  $-0.88 \pm 0.27 \text{‰}$  ( $1\sigma$ ; for the Pacific Ocean). The Southern and Indian Oceans have a more restricted range than the Atlantic and the Pacific, but this is probably due to more limited sampling, especially for the Southern Ocean which is represented by only two samples. The standard deviations of the mean for the Atlantic and Pacific Ocean samples are nearly equal and the data largely overlap. It is difficult to conclude if the bias of the Atlantic samples toward heavier values and of the Pacific samples toward somewhat lighter values is a real difference or just an artefact of number and density of sampling. Most of the samples at the ocean margins have very light compositions and a larger fraction of the Pacific Ocean samples are from oceanic margins. A comparison of the Fe isotope

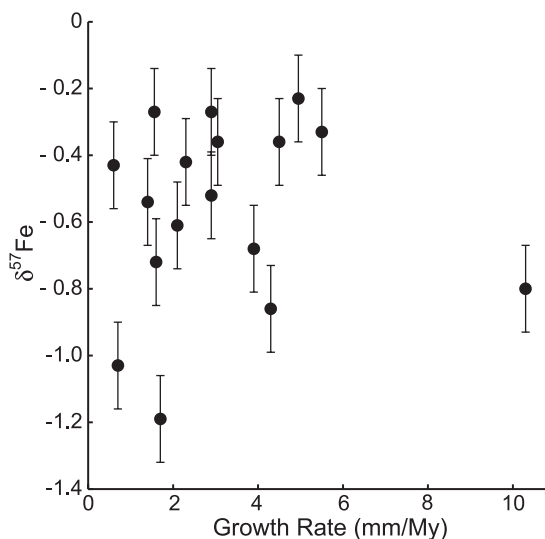


Fig. 2.  $\delta^{57}\text{Fe}$  [‰; (●)] as a function of the growth rate in hydrogenous crusts. The error bars are  $0.13 \text{‰}$  ( $2\sigma$ ).

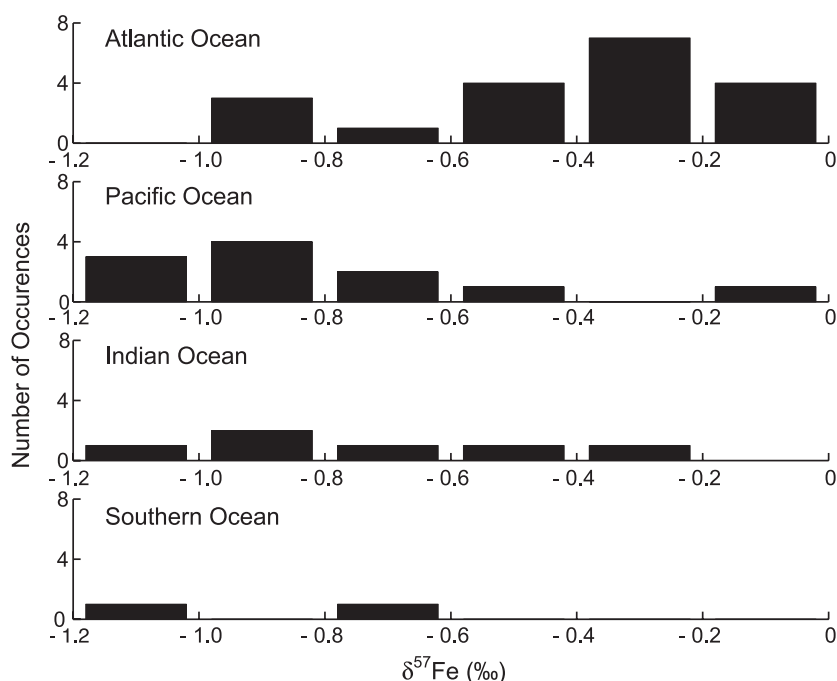


Fig. 3. Histogram showing the distribution of  $\delta^{57}\text{Fe}$  compositions for all samples for each ocean.

compositions with the Pb and Nd isotope compositions (Fig. 4) available from the same crusts shows no obvious correlation with either of these tracers. Furthermore, no correlation with Fe/Mn ratio or other elemental or mineralogical parameters in the crusts, water depth or proximity to midoceanic ridges is visible.

## 4. Discussion

### 4.1. Source effects

#### 4.1.1. Continental sources

Zhu et al. [4] found a correlation between Fe and Pb isotopic compositions in a 6 Myr time series in North Atlantic crust BM1969.05 [Fig. 5c, (O)]. They concluded that Fe isotope variations in seawater were correlated with other better-understood parameters such as Pb isotopes which reflect the weathering of continental sources [3].

The correlation between Fe and Pb isotopes in BM1969.05 is predominantly defined by the most recent data point of the time series. We have rean-

alysed a different slab of this crust and found the surface data point previously measured at  $+0.2\text{‰}$  in  $\delta^{57}\text{Fe}$  to instead yield a value of  $-0.75\text{‰}$ . To check that we had really analysed the same time slice as Zhu et al. [4], we also measured the Pb isotope composition and found a composition of 19.21 in  $^{206}\text{Pb}/^{204}\text{Pb}$ , which is comparable to that previously reported. The high gradient of Pb isotope change in the upper part of the crust unambiguously shows that the sections and the depth of the sub-sample measured by us and by Zhu et al. [4] are essentially identical. We then measured older parts of the crust (0.5 to 0.8 mm depth and 0.8 to 1.6 mm) and again found values that are lower than those reported previously:  $-0.58$  and  $-0.78\text{‰}$ . We do not have a clear explanation for this discrepancy. One possibility is that different portions of the surface of the crust yield different Fe isotopic compositions, although this is not supported by our other analyses of different samples from the same crusts (e.g., D140-3 or D219-7). There is also not a systematic interlaboratory discrepancy between the measurements: the differences are variable and we find the same composition as reported by Zhu et al.



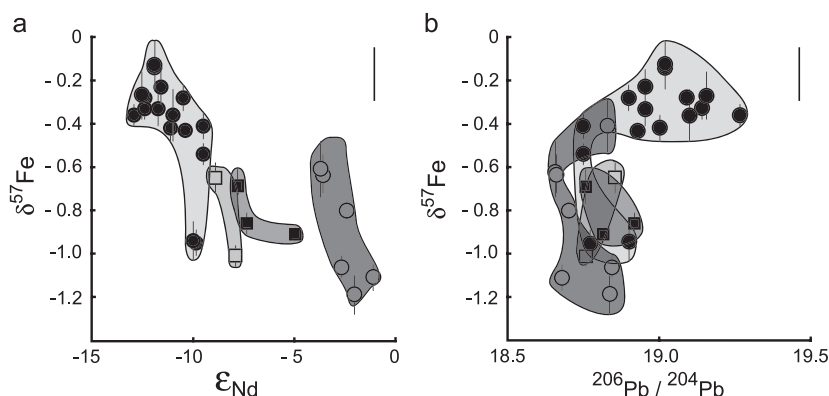


Fig. 4.  $\delta^{57}\text{Fe}$  as a function of (a)  $\epsilon_{\text{Nd}}$  and (b)  $^{206}\text{Pb}/^{204}\text{Pb}$  in hydrogenous crusts. The error bars are  $2\sigma$  (three to eight measurements). The error bar in the upper right-hand corners of the panels is the  $2\sigma$  long-term reproducibility on  $\delta^{57}\text{Fe}$ . Dots = Atlantic Ocean; squares = Southern Ocean; black squares = Indian Ocean; circles = Pacific Ocean.

[4], supplementary material) for the iron meteorite Tazewell (0.22‰ vs. 0.20‰ for Zhu et al.). One thing that could be significant is that we do not observe an evolution of the isotopic composition of Fe over months when stored in dilute HCl (0.05 N) as reported by [11]. We have reanalysed samples up to 6-months interval without seeing significant differences. We have also reprocessed a fraction of some samples after 11 months of storage in dilute HCl through new column chemistry (without any oxidation step), and no fractionation was observable.

If one uses the new data presented here the correlation between Pb and Fe isotopes breaks down (Fig. 4c). Therefore, the main line of evidence that the Fe isotope composition in BM1969.05 is related to variations in terrigenous inputs cannot be reproduced with the data we have obtained.

The absence of a correlation between Pb or Nd and Fe isotopes in the ferromanganese crust surfaces representing the present-day oceans (Fig. 3), as well as the remarkable homogeneity of Fe isotopes in igneous and sedimentary rocks [7,12], are additional evidence against a causal relationship between the variations of Fe isotope compositions in ferromanganese crusts and the putative variations in source rocks and/or weathering processes on the surrounding continents.

#### 4.1.2. Mixing between continental and hydrothermal

#### sources

If the variation in the Fe isotope composition of ferromanganese crust surfaces does not reflect variability in terrigenous inputs, the question arises as to what other processes or inputs could be responsible. Sharma et al. [13] have suggested that such variation could be due to variations in the proportions of Fe derived from the hydrothermal inputs at midoceanic ridges (MORs) and of Fe coming from the continents. This was based on the observation that fluids emanating from hydrothermal vents at the Juan de Fuca Ridge are lighter than the terrestrial baseline ( $-0.2$  to  $-0.9$ ‰  $\delta^{57}\text{Fe}$ , renormalized to IRMM-14 from the Canyon Diablo meteorite normalization used in [13]). Sharma et al. [13] proposed that light Fe emerging from the ridge vents would experience further isotope fractionation during processes of Fe removal because laboratory studies [14] demonstrated that precipitation of ferrihydrite from dissolved  $\text{Fe}^{2+}$  is accompanied by a fractionation of 1‰, favouring heavy Fe in the precipitate. This would lead to increasingly negative  $\delta^{57}\text{Fe}$  in seawater and in sediments with increasing distance from ridge axes. The Fe isotope composition of  $-1.69$ ‰ (Table 1) for the hydrothermal deposit from the Galapagos ridge (Pleiade II, D5-1A) agrees with the isotopic composition suggested by Sharma et al. [13]. However, the data for hydrogenous crusts show no relation between Fe isotope composition and distance to oceanic ridges (Fig. 1).

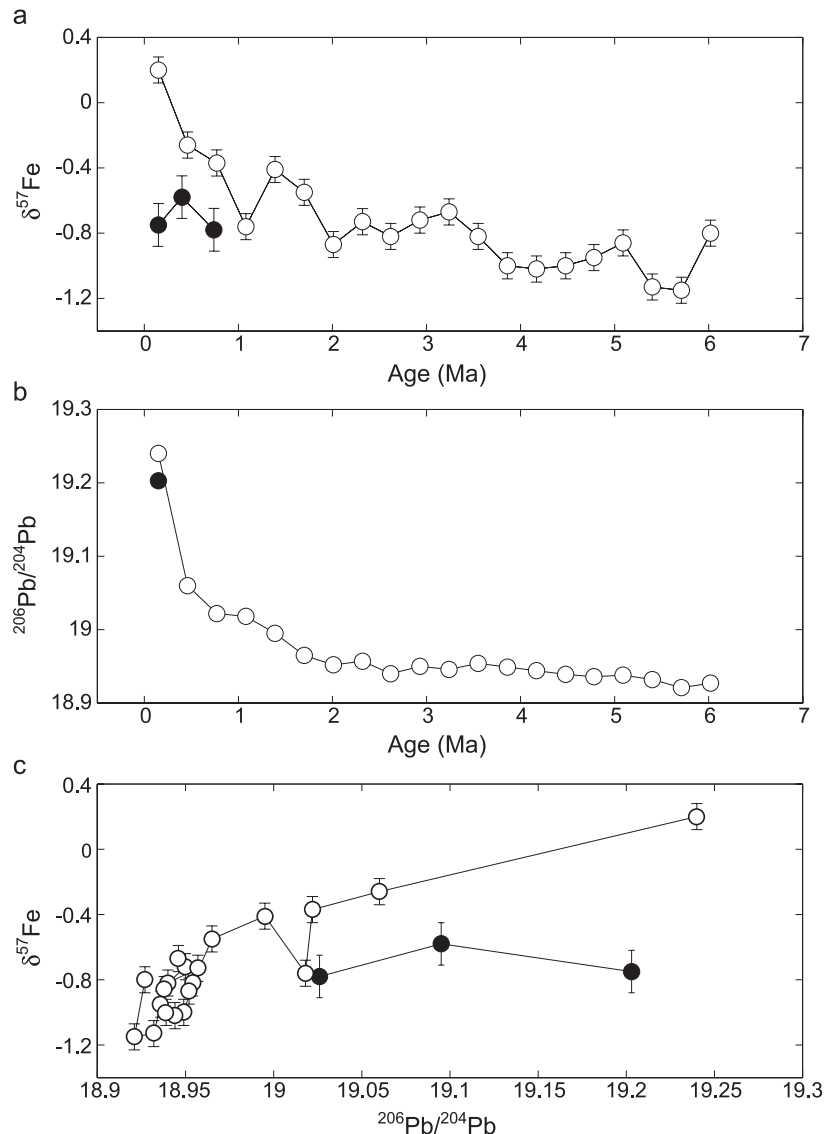


Fig. 5. Variations with time of  $\delta^{57}\text{Fe}$  (a),  $^{206}\text{Pb}/^{204}\text{Pb}$  (b) and  $\delta^{57}\text{Fe}$  as a function of  $^{206}\text{Pb}/^{204}\text{Pb}$  (c) in crust BM1969.05 (northeast Atlantic Ocean) obtained by Zhu et al. [4] (○) and by this study (●). The lead values used for the samples at depth 0.5–0.8 and 0.8–1.6 are extrapolated from [4] (Supplementary material). The error bars for the present data are  $2\sigma$  long-term reproducibility of a hematite sample used as our lab standard. For the data from [4], the error bars are the reproducibility of repeated measurements of Aldrich Fe solution during the run.

Recently, Beard et al. [12] have measured seven MOR hydrothermal fluids from the Atlantic and Pacific Oceans, with an improved precision, and found a  $\delta^{57}\text{Fe} = -0.44 \pm 0.18\text{‰}$ . According to them, the Fe delivered to the oceans is essentially controlled by the atmospheric particulate flux and the MOR hydrothermal flux (respectively 67% and 23%

on average), but because the proportion of the atmospheric flux is variable between ocean basins, they calculate various Fe isotopic compositions for the different basins by assuming simple mixing between the two components. A way to test this model is to plot the results we obtained for ferromanganese crusts on the diagram representing the model (Fig. 6) using

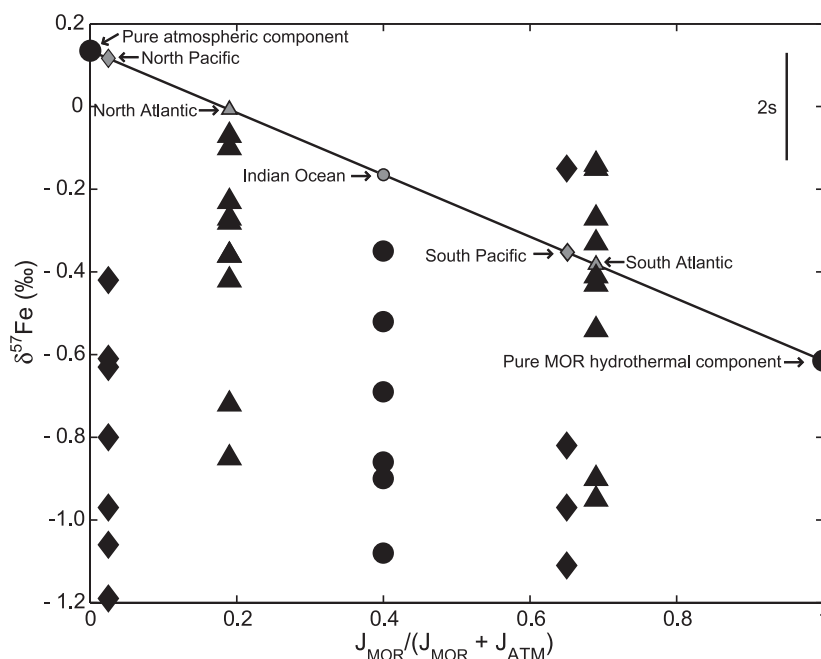


Fig. 6.  $\delta^{57}\text{Fe}$  of the hydrogenic crusts analysed in this study superimposed to the model from [12]. Calculated Fe isotope composition of seawater from different oceans based on simple two-component mixing between Fe from aerosol particles and Fe from midoceanic ridge (MOR). The  $\delta^{57}\text{Fe}$  of this lower component is set at the lower range of the estimated variability of hydrothermal fluids:  $-0.44$ –

the mixing proportions proposed for the different basins. It is obvious that the data do not fit the model and that nearly half of the data cannot fit a simple mixing line whatever the mixing proportion, as their composition is lower than that of the hydrothermal component. There could be different reasons for this discrepancy:

- (1) There is a fractionation process during the incorporation of Fe from seawater into the ferromanganese crusts. Such an effect has already been observed for Tl isotopes [15].
- (2) The model is not correct and the composition of Fe in seawater is not controlled by the mixture of the atmospheric particulate component and the MOR hydrothermal component.
- (3) Hypotheses (1) and (2) both apply.

Although (1) probably contributes to the observed Fe isotope distribution (see below), it is highly probable that (2) applies and that the model is incorrect. In their calculations, Beard et al. [12] used a flux of hydrothermal Fe equal to  $10^{13}$  g/year. This is

at the high end of the range ( $1.3$ – $11 \times 10^{12}$  g/year) determined by the reference they used [16], which is also similar to a more recent estimate ( $1.7$ – $5 \times 10^{12}$  g/year) [17]. If the flux were at the lower end of the range, the proportion of Fe coming from the hydrothermal component would be reduced to 3% or 4% instead of 23%. The main problem of this model, however, is not the uncertainty over the initial magnitude of the hydrothermal flux. It is the fact that it ignores the vast loss of such hydrothermal Fe in and around vents. The reduced Fe precipitates very rapidly in the form of sulfides and hydroxides. Although the oxidation rate of hydrothermal Fe(II) seems to be variable as a consequence of the ambient deepwater conditions, the maximum half-life of Fe(II) is a few hours and the concerned area is thus limited to a few kilometers from the vent sites [18]. Thereafter, little of the original Fe remains in solution in seawater [17]. More than 90% of hydrothermal Fe is lost in this manner and is not contributed to the budget of dissolved Fe that enters the ocean. Therefore, a conservative estimate of the net input of Fe from hydrothermal sources into deep ocean water would

be, at the global scale, between 2.9% and 0.4% of the total Fe to the ocean. This, a very small amount compared with input from the continents. Traces of hydrothermal Fe can be found in sediments at larger distances from ocean ridges, for example, several hundreds kilometers west of the East Pacific Rise [19]. However, this is due to transport of the colloidal lower end of the size fraction of oxyhydroxide iron particles that form during the oxidation of Fe(II). It does not imply a mixture of soluble hydrothermal Fe(II) within the ocean. In fact, the presence of hydrothermal particles at such distances is not the rule but is dependent on the topography and prevalent circulation patterns. Unlike the observation for the Pacific, the plume that forms above the TAG hydrothermal vent field stays confined within the axial valley of the mid-Atlantic Ridge [20].

Of course, the above discussion, as well as the model of Beard et al. [12], neglects low-temperature hydrothermal activity at ridge flanks. Whether such activity provides a source or sink of iron is very poorly known, to say nothing of the flux. A recent review of the fluxes at ridge flanks [21] concluded that Fe fluxes are zero albeit with large uncertainties.

Finally, the samples studied here are hydrogenous. Thus, the only way to have a hydrothermal component in the crusts would be to homogenize it with the other Fe sources in the ocean. As the residence time of Fe in seawater is very short (70–200 years, e.g., [22]), this should only be of regional importance although it may be possible that mixing processes in the deep waters are somewhat more efficient than surface waters in redistributing hydrothermal Fe. Therefore, we conclude that there is no evidence that hydrothermal inputs play an important role in the large-scale budgets and isotopic compositions of Fe in the oceans and that its importance is probably geographically limited.

#### 4.1.3. *Admixing of diagenetic components*

It has been argued [17] that in some oceanic areas, the diagenetic input (remobilisation of Fe from the bottom sediments) could be a source of Fe of some importance in bottom waters. In fact, some manganese nodules are known to form from this remobilised material, and for this reason, they are called diagenetic–hydrogenous deposits. However, for a set of samples from the central Pacific, it has been established that the substrate rocks, on

which crusts grow, and the associated pore fluids do not contribute to the composition of hydrogenous ferromanganese crusts [23]. Thus, the fraction of diagenetic material in surface layers of hydrogenous crusts is negligible.

#### 4.2. *Internal processes in ocean basins*

If the isotopic variations do not reflect source variations or mixing of sources, the possibility needs to be considered that the Fe isotopic variations are caused by fractionation at some point between the introduction of Fe into the ocean and the incorporation into the crusts.

The main particulate sources that contribute Fe to the oceans are rivers and eolian dust. The largest source of particulate Fe are rivers but most of the particulates are deposited near shore and do not contribute to the open ocean budget. The second source is wet and dry deposition of continental aerosols [17].

In rivers, most of the dissolved Fe is present as small colloidal particles. During estuarine mixing, these colloids flocculate, and in most cases, do not escape the estuary. Therefore, they do not contribute notably to the Fe input to the ocean, although they could be locally important [24].

The main source of dissolved Fe seems to be the reductive remobilisation of Fe in marine sediments, although this still needs to be quantified [17]. Coastal sediments can give rise to huge Fe fluxes when they turn anoxic after the spring bloom has settled to the seafloor [25], and this could certainly induce an isotopic fractionation of Fe. The reducing process and the dissolution followed by partial readsorption and precipitation on suspended particles of the newly dissolved Fe are all processes that might potentially fractionate the remaining Fe, which stays longer in solution, toward lighter values. This remobilised Fe could have a regional influence once mixed in the water masses.

The second largest source is the reductive dissolution of eolian particles during wet deposition [17]. The total eolian input is estimated to be about 70% via dry and about 30% via wet deposition. Subsequent dissolution in seawater seems to be negligible for dry deposition [26] whereas  $\sim 14\%$  of Fe in wet deposition is dissolved in rainwater. This dissolution step could already be a source of fractionation as suggested by [12]. A large part of these, 14% is reprecipitated in

the surface ocean so that Fe solubility through this process is probably less than 2% [26]. The bulk eolian input of Fe to the ocean should have an iron isotope composition similar to that of continental rocks. However, only a small fraction of it will finally be dissolved in seawater, 90–99% of which will be in the upper water column as Fe(III), complexed with strong Fe-binding organic ligands [27].

This step of dissolution and complexation by organic ligands can very probably be a source of isotopic fractionation toward lighter values. Brantley et al. [28] showed that siderophores produced by bacterial dissolution of silicate soil minerals are as much as 0.8‰ lighter than bulk Fe in the original mineral. Although the nature of the Fe(III)-binding ligands in seawater is not well established, it has been shown that their binding strength is very similar to those of siderophores produced by marine bacteria [29] and that they possess functional group characteristics of siderophores [30]. If we assume that these ligands are siderophores and we extrapolate the result obtained by Brantley et al. [28] to seawater, then the dissolution of Fe from eolian dust by means of organic ligands could be an important source of fractionation toward lighter values. Even if these organic molecules were not siderophores, but, for example, products of the decomposition of planktonic microorganisms, it would not change the conclusion that the fractionation appears to be related to the binding strength of the ligand [28]. This is consistent with the behaviour found for Zn isotopes in surface seawater [31] where the lighter isotopes are preferentially used by biological activity. Following the case of the Zn, it is possible that remineralisation plays a role in the isotopic variability [31] of Fe observed in the ferromanganese crusts; however, data are lacking to ascertain this.

These different mobilisation processes of Fe in different oceanic areas could possibly explain why ocean margin samples, where the anoxic dissolution from sediments is certainly a dominant process, tend to show a distinct composition compared to other regions.

This does not preclude the possibility of other fractionation processes in the course of cycling of Fe through the ocean, especially during the incorporation of Fe into the ferromanganese crust *per se*. This has already been observed for the isotopes of other heavy elements like Tl [15], where a 2‰

enrichment in the heavy isotope occurs between seawater and ferromanganese particles during adsorption; or like Mo [32], where a similar 2‰ enrichment takes place, but this time, in favour of the incorporation of the light isotopes. Surface adsorption and ion exchange processes produce isotopic fractionation for Fe in experimental systems [33] so this hypothesis is quite plausible. If this is the case, it should be expected that the dissolved Fe in the surrounding seawater is shifted compared to what we observed in the crust.

Mineralogically, ferromanganese crusts consist of manganese oxides ( $\delta$ -MnO<sub>2</sub>), amorphous Fe oxyhydroxides (FeOOH) and minor detrital minerals. Leaching experiments have shown that between 30% and 50% of the total Fe is present as FeOOH intergrown with the Mn oxide in the vernadite 10% to 30% [34]; most of the remainder being discrete FeOOH. Temperature effects can be ruled out as a source of variable fractionations from one crust to another due to the small temperature range of deep seawater. However, it is possible that some fractionation could be induced by the variable amount of FeOOH intergrown with Mn oxide and redox reactions at crust surfaces. If there is such a process, the seawater pool could be expected to be more homogeneous than what is observed in the crusts. Of course, this does not preclude the possibility of regional heterogeneity reflecting the short residence time and the varying degrees of fractionation associated with inputs to a given region.

## 5. Conclusions

New measurements of Fe isotopic compositions in hydrogenous crusts distributed throughout the world oceans confirm that although there is a large range in composition, this range has a similar average for each main ocean basin, and no significant basin-to-basin trend is discernable.

Our data do not substantiate evidence that purports to show that Fe isotope compositions that are coupled with Pb or Nd isotope compositions. Indeed, the data presented here provide evidence that isotopic composition of Fe is not driven by variations in continental source composition. Furthermore, the minor amount of Fe coming from hydrothermal sources as well as

the very small amount of hydrothermal Fe incorporated in hydrogenous crusts seems to preclude the possibility that variable mixtures of hydrothermal and continental Fe result in large-scale variations in Fe isotopic composition. Further constraints are needed in order to establish exactly what are the most likely explanations for the fractionations that take place during geochemical and biogeochemical reactions within the ocean. All of these could play a role in establishing the isotopic composition that we find in ferromanganese crusts. To determine which of these processes is preponderant or at least relevant to the isotope fractionation observed in hydrogenous ferromanganese crusts requires additional studies.

## Acknowledgements

We thank the Scripps Institution of Oceanography, the Oregon State University and the Woods Hole Oceanographic Institution for supplying several crusts. We acknowledge the careful reviews and useful comments of H. de Baar, J.-M. Luck, F. Albarède and R. Sherrell. We want to thank the Swiss National Science Foundation (SNSF) and ETH for financial support of this work. *[BARD]*

## References

- [1] J.H. Martin, S.E. Fitzwater, Iron deficiency limits phytoplankton growth in the north east Pacific subarctic, *Nature* 331 (1988) 341–343.
- [2] D.R. Turner, K.A. Hunter, *The Biogeochemistry of Iron in Seawater*, Wiley, Chichester, 2001.
- [3] M. Frank, Radiogenic isotopes: tracers of past ocean circulation and erosional input, *Rev. Geophys.* 40 (2002) DOI:10.1029/2000RG000094.
- [4] X.-K. Zhu, K. O’Nions, Y. Guo, B.C. Reynolds, Secular variation of iron isotopes in North Atlantic deep water, *Science* 287 (2000) 2000–2002.
- [5] X.-K. Zhu, Y. Guo, K. O’Nions, Spatial and temporal variations of transition metal isotopes in oceans, *Goldschmidt Conf. Abstracts, Geochim. Cosmochim. Acta*, vol. 66, 2002, p. A880, Davos, Switzerland.
- [6] M. Frank, B.C. Reynolds, R.K. O’Nions, Nd and Pb isotopes in Atlantic and Pacific water masses before and after the closure of the Panama gateway, *Geology* 27 (1999) 1147–1150.
- [7] C.M. Johnson, B.L. Beard, N.J. Beukes, C. Klein, J.M. O’Leary, Ancient geochemical cycling in the Earth as inferred from Fe isotope studies of banded iron formations from the Transvaal Craton, *Contrib. Mineral. Petrol.* 144 (2003) 523–547.
- [8] M. Frank, R.K. O’Nions, J.R. Hein, V.K. Banakar, 60 Myr records of major elements and Pb–Nd isotopes from hydrogenous ferromanganese crusts: reconstruction of seawater paleochemistry, *Geochim. Cosmochim. Acta* 63 (1999) 1689–1708.
- [9] N.S. Belshaw, X.-K. Zhu, Y. Guo, R.K. O’Nions, High precision measurement of iron isotopes by plasma source mass spectrometry, *Int. J. Mass Spectrom.* 197 (2000) 191–195.
- [10] B.L. Beard, C.M. Johnson, J.L. Skulan, K.H. Nealson, L. Cox, H. Sun, Application of Fe isotopes to tracing the geochemical and biological cycling of Fe, *Chem. Geol.* 195 (2003) 87–117.
- [11] X.K. Zhu, Y. Guo, R.J.P. Williams, R.K. O’Nions, A. Matthews, N.S. Belshaw, G.W. Canters, E.C. de Waals, U. Weser, B.K. Burgess, B. Salvato, Mass fractionation processes of transition metal isotopes, *Earth Planet. Sci. Lett.* 200 (2002) 47–62.
- [12] B.L. Beard, C.M. Johnson, K.L. Von Damm, R.L. Poulson, Iron isotope constrains on Fe cycling and mass balance in the oxygenated earth, *Geology* 31 (2003) 629–632.
- [13] M. Sharma, M. Polizzotto, A.D. Anbar, Iron isotopes in hot springs along the Juan de Fuca Ridge, *Earth Planet. Sci. Lett.* 194 (2001) 39–51.
- [14] T.D. Bullen, A.F. White, C.W. Childs, D.V. Vivit, M.S. Schulz, Demonstration of significant abiotic iron isotope fractionation in nature, *Geology* 29 (2001) 699–702.
- [15] M. Rehkamper, M. Frank, J.R. Hein, D. Porcelli, A. Halliday, J. Ingri, V. Liebetrau, Thallium isotope variations in seawater and hydrogenetic, diagenetic, and hydrothermal ferromanganese deposits, *Earth Planet. Sci. Lett.* 197 (2002) 65–81.
- [16] H. Elderfield, A. Schultz, Mid-ocean ridge hydrothermal fluxes and the chemical composition of the ocean, *Annu. Rev. Earth Planet. Sci.* 24 (1996) 191–224.
- [17] H.J.W. De Baar, J.T.M. De Jong, Distributions, sources and sinks of iron in seawater, in: D.R. Turner, K.A. Hunter (Eds.), *The Biogeochemistry of Iron in Seawater*, Wiley, Chichester, 2001, pp. 124–234.
- [18] M.P. Field, R.M. Sherrell, Dissolved and particulate Fe in a hydrothermal plume at 9°45’ N, East Pacific Rise: slow Fe(II) oxidation kinetics in Pacific plumes, *Geochim. Cosmochim. Acta* 64 (2000) 619–628.
- [19] M.W. Lyle, Major element composition of LEG 92 sediments, in: M. Leinen, D.K. Rea, et al. (Eds.), *Init. Repts. DSDP, 92*, U.S. Govt. Printing Office, Washington, 1992.
- [20] M.D. Rudnicki, H. Elderfield, A chemical model of the buoyant and neutrally buoyant plume above the TAG vent field, 26 degrees N, mid-Atlantic ridge, *Geochim. Cosmochim. Acta* 57 (1993) 2939–2957.
- [21] J.C. Alt, Hydrothermal fluxes at mid-ocean ridges and on ridge flanks, *C. R. Geosci.* 335 (2003) 853–864.
- [22] K.S. Johnson, R.M. Gordon, K.H. Coale, What controls dissolved iron concentrations in the world ocean? *Mar. Chem.* 57 (1997) 137–161.
- [23] J.R. Hein, C.L. Morgan, Influence of substrate rocks on Fe–Mn crust composition, *Deep-Sea Res.* 46 (1999) 855–875.
- [24] R.T. Powell, A. Wilson-Finelli, Importance of organic Fe complexing ligands in the Mississippi River plume, *Estuarine*,



- Coast. Shelf Sci. 58 (2003) 757–763.
- [25] V. Schoemann, H.J.W. de Baar, J.T.M. de Jong, C. Lancelot, Effects of phytoplankton blooms on the cycling of manganese and iron in coastal waters, *Limnol. Oceanogr.* 43 (1998) 1427–1441.
- [26] T.D. Jickells, L.J. Spokes, Atmospheric iron inputs to the oceans, in: D.R. Turner, K.A. Hunter (Eds.), *The Biogeochemistry of Iron in Seawater*, Wiley, Chichester, 2001, pp. 85–121.
- [27] E.L. Rue, K.W. Bruland, Complexation of iron(III) by natural organic ligands in the central North Pacific as determined by a new competitive ligand equilibration/adsorptive cathodic stripping voltammetric method, *Mar. Chem.* 50 (1995) 117–138.
- [28] S.L. Brantley, L. Liermann, T.D. Bullen, Fractionation of Fe isotopes by soil microbes and organic acids, *Geology* 29 (2001) 535–538.
- [29] J.W. Moffett, Transformations among different forms of iron in the ocean, in: D.R. Turner, K.A. Hunter (Eds.), *The Biogeochemistry of Iron in Seawater*, Wiley, Chichester, 2001, pp. 343–372.
- [30] H.M. Macrellis, C.G. Trick, E.L. Rue, G. Smith, K.W. Bruland, Collection and detection of natural iron-binding ligands from seawater, *Mar. Chem.* 76 (2001) 175–187.
- [31] C.N. Marechal, E. Nicolas, C. Douchet, F. Albarede, Abundance of zinc isotopes as a marine biogeochemical tracer, *Geochim. Geophys. Geosystems* 1 (2000) DOI:1999GC000029.
- [32] J. Barling, A.D. Anbar, Molybdenum isotope fractionation during adsorption by manganese oxides, *Earth Planet. Sci. Lett.* 217 (2004) 315–329.
- [33] A.D. Anbar, J.E. Roe, J. Barling, K.H. Nealson, Nonbiological fractionation of iron isotopes, *Science* 288 (2000) 126–128.
- [34] A. Koschinsky, J.R. Hein, Uptake of elements from seawater by ferromanganese crusts: solid-state associations and seawater speciation, *Mar. Geol.* 198 (2003) 331–351.
- [35] G.M. Henderson, K.W. Burton, Using ( $^{234}\text{U}/^{238}\text{U}$ ) to assess diffusion rates of isotope tracers in ferromanganese crusts, *Earth Planet. Sci. Lett.* 170 (1999) 169–179.
- [36] B.C. Reynolds, M. Frank, R.K. O’Nions, Nd- and Pb-isotope time series from Atlantic ferromanganese crusts: implications for changes in provenance and paleocirculation over the last 8 Myr, *Earth Planet. Sci. Lett.* 173 (1999) 381–396.
- [37] R.K. O’Nions, M. Frank, F. von Blanckenburg, H.-F. Ling, Secular variation of Nd and Pb isotopes in ferromanganese crusts from the Atlantic, Indian and Pacific Oceans, *Earth Planet. Sci. Lett.* 155 (1998) 15–28.
- [38] M. Frank, T. van de Flierdt, A.N. Halliday, P.W. Kubik, B. Hattendorf, D. Günther, Evolution of deepwater mixing and weathering inputs in the central Atlantic Ocean over the past 33 Myr, *Paleoceanography* 18 (2003) DOI:10.1029/2003PA000919.
- [39] F. Chabaux, R.K. O’Nions, A.S. Cohen, J.R. Hein,  $^{238}\text{U}$ – $^{234}\text{U}$ – $^{230}\text{Th}$  disequilibrium in hydrogenous oceanic Fe–Mn crusts: palaeoceanographic record or diagenetic alteration? *Geochim. Cosmochim. Acta* 61 (1997) 3619–3632.
- [40] M. Frank, N. Whiteley, S. Kasten, J.R. Hein, K. O’Nions, North Atlantic deep water export to the southern ocean over the past 14 Myr: evidence from Nd and Pb isotopes in ferromanganese crusts, *Paleoceanography* 17 (2002) DOI:10.1029/2000PA000606.
- [41] T. van de Flierdt, M. Frank, A.N. Halliday, J.R. Hein, B. Hattendorf, D. Günther, P.W. Kubik, Lead isotopes in North Pacific deep water—implications for past changes in input sources and circulation patterns, *Earth Planet. Sci. Lett.* 209 (2003) 149–164.